Food and Bioprocess Technology
https://doi.org/10.1007/s11947-023-03296-7

RESEARCH

Development of O/W Pickering Emulsions Stabilized with Leek Leaf Trimmings Using Batch and Continuous Modes

M. P. Marques[1,2] · J. L. Sanchez-Salvador[3] · M. C. Monte[3] · A. Blanco[3] · R. J. Santos[1,2] · M. M. Dias[1,2] · Y. A. Manrique[1,2] · M. S. C. A. Brito[2,4]

Received: 28 August 2023 / Accepted: 11 December 2023

Abstract

Vegetable trimmings can be used to stabilize edible O/W Pickering emulsions. The lignocellulosic biomass (LCB) from the leek trimmings was mechanically treated to produce high-yield lignocellulose micro and nanofibrils (LCF) using a high-pressure homogenizer (HPH). Different O/W phase ratios (20/80, 30/70, and 40/60 wt.%) were studied. The use of the micro/nano cellulosic fibers increased the stabilization of the Pickering emulsions by 30–40%. In all cases, stable emulsions were obtained, with emulsification indexes > 92%. The respective stabilization mechanism was thoroughly analysed from confocal laser scanning, and cryo-scanning electron microscopy, which showed the fibers are not coating the droplets but forming a network that traps the droplets and prevents coalescence. The most stable batch formulations, O/W 30/70 wt.% (LCB 4.2 wt.%) and O/W 40/60 wt.% (LCB 3.6 wt.%), were also studied in continuous mode using NETmix technology. Results show the scale-up feasibility of the production of Pickering emulsions containing LCF. Most significantly, this work proposes a continuous process to produce Pickering emulsions stabilized with a natural biopolymer extracted from leek trimmings, which is suitable to industrial manufacturing processes. This valorizes the vegetable trimmings that are usually tossed away as waste, creating new market niches and business models based on circular economy concepts.

Keywords Pickering emulsions · Lignocellulosic biomass · Fibrillated cellulose · Micro/nanofibers NETmix Technology · Leek residues

Introduction

Vegetable trimmings produced in greengroceries, when not consumed during their lifespan, are mostly tossed away as waste. If this waste is not treated, several environmental problems may arise (e.g. production of nitrous oxide, methane, sulfur dioxide, smoke). Alternatively, the burning of these residues results in carbon dioxide emissions, contributing to atmospheric pollution (He et al., 2020; Jimenez-Lopez et al., 2020; Rao & Rathod, 2019).

These vegetable trimmings are lignocellulosic biomass (LCB) composed of cellulose, hemicellulose, and lignin (Balea, 2017). Therefore, there is a significant interest in finding circular economy processes to obtain new high value-added products for the food industry from this type of wastes (Mateo et al., 2021; Sanchez et al., 2023). Cellulose has been recently used in Pickering emulsions, showing its potential as stabilizer for edible use or as alternative to traditional surfactants for other applications (Costa et al., 2018; Li, Li et al., 2019; He et al., 2020).

Pickering emulsions, which were introduced at the beginning of the twentieth century by Ramsden and Pickering, use solid particles to form a thick barrier at the oil/water (O/W) interface. These particles act as an obstacle against the coalescence of droplets (Pickering, 1907), thus avoiding the use

✉ M. S. C. A. Brito
mbrito@fe.up.pt

1 Laboratory of Separation and Reaction Engineering–Laboratory of Catalysis and Materials (LSRE-LCM), Faculty of Engineering, University of Porto, Rua Dr. Roberto Frias, 4200-465 Porto, Portugal

2 ALiCE–Associate Laboratory in Chemical Engineering, Faculty of Engineering, University of Porto, Rua Dr. Roberto Frias, 4200-465 Porto, Portugal

3 Chemical Engineering and Materials Department, Universidad Complutense de Madrid (UCM), Avda. Complutense s/n, 28040 Madrid, Spain

4 Laboratory of Process Engineering, Environment, Biotechnology and Energy (LEPABE), Faculty of Engineering, University of Porto, Rua Dr. Roberto Frias, 4200-465 Porto, Portugal

Published online: 18 January 2024

of surfactants. Pickering emulsions can be oil-in-water and water-in-oil emulsions. Oil-in-water emulsions are characterized by the formation of oil droplets in an aqueous continuous phase, and the opposite behaviour occurs for water-in-oil emulsions. The type of emulsion formed depends mainly on the wettability of the particles, characterized by the three-phase contact angle measured through the water phase (θ). Hydrophilic particles ($\theta < 90°$) usually stabilize oil-in-water emulsions, whereas hydrophobic particles ($\theta > 90°$) lead to water-in-oil emulsions (Binks & Lumsdon, 2000).

Due to their surfactant-free character, some applications of Pickering emulsions, such as in pharmaceutics (Albert et al., 2019; Zongguang et al., 2020), cosmetics (Marto et al., 2020; Sharkawy et al., 2021), and food (Sanchez-Salvador et al., 2019; Chen et al., 2020), are gaining increasing attention. Their attractiveness relates to the possibility of using solid organic particles obtained from natural sources, with good biocompatibility, biodegradability, and nontoxicity. Natural organic Pickering stabilizers include starch particles (Li et al., 2013; Ye et al., 2017), chitin nanocrystals (Tzoumaki et al., 2011), protein particles (de Folter et al., 2012; Liang & Tang, 2014; Jiang et al., 2019; Liu et al., 2020), peptides nanoparticles (Sharkawy et al., 2021; Zhang et al., 2022), dietary fiber (Chen et al., 2023), linear polysaccharides such as dextran (Maingret et al., 2020) or alginate (Rescignano et al., 2015), rocket and chia seed gum nanoparticles (Akcicek et al., 2022), apple pomace (Lu et al., 2020), and other cellulose products.

Cellulose successfully stabilizes Pickering emulsions due to its amphiphilic nature. These fibers have a hydrophobic face and a hydrophilic edge, enabling them an adequate position at the O/W interface and prevent the coalescence of droplets (Sanchez-Salvador et al., 2019). Saffarionpour (2020) gives an overview of the previous works on the production of Pickering emulsions using cellulose that have less toxic effects in the gastrointestinal tract than the traditional surfactants. These emulsions can be prepared to encapsulate neutraceuticals achieving a controlled release in the gastrointestinal tract. Cellulose products obtained from LCB used as Pickering stabilizers include cellulose micro and nanofibers (CMFs, CNFs) from oil palm empty fruit bunch waste (Li, Li et al., 2019), banana peels (Costa et al., 2018), and bamboo shoot (He et al., 2020). However, CNFs are produced by mechanical fibrillation in expensive low-yield processes (Balea Martin et al., 2021; Blanco et al., 2018; Negro et al., 2020). In most cases, a chemical pre-treatment is used to reduce energy costs which limits their application for food and cosmetics (Chen et al., 2021). Sanchez-Salvador et al. (2019) report the use of chemically untreated cotton linters (> 99.9% cellulose) for CMF production as Pickering particles compatible with food application. LCB without chemical pre-treatments from wet-milled apple pomace particles has been used to study the influence of particle size at 50/50 wt.% O/W ratio (Lu et al., 2020). Tomato pomace fibrillated by HPH has also been used for emulsification (Pirozzi et al., 2021). Recently, LCB containing micro and nanofibrils was successfully obtained from leek, lettuce, and artichoke trimmings at highly concentrated suspensions (5–5.5 wt.%) (Sanchez-Salvador et al., 2022). The presence of lignin and hemicellulose along with cellulose is beneficial for emulsion's stability. Hemicellulose increases the viscosity of the dispersion phase, which, according to the Stokes Law, proportionally decreases the separation rate of the immiscible liquids (Olorunsola et al., 2018). Lignin, which is less hydrophilic than cellulose, reduces the overall hydrophilic properties of the fibers resulting in better oil-in-water emulsion stability (Guo et al., 2021).

Yuan et al. (2021) report that the mechanical treatments to produce cellulosic fibers affect the morphological properties and then the stabilization of O/W emulsions. The aspect ratio and the fibrillation degree that controls the fibers' size and shape are the main parameters that affect the emulsions' stabilization mechanisms. Kalashnikova et al. (2013) studied the impact in the stabilization mechanisms of aspect ratio in a range from 13 to 60. When CNFs have a small aspect ratio, their behaviour is similar to cellulose nanocrystals, i.e. the particles are absorbed at the interface reducing the interfacial area (Miao et al., 2020). When the aspect ratio is large, CNFs exclude the region next to the oil interface due to depletion interactions, inducing the flocculation of oil droplets. On the other hand, the degree of fibrilization is related to the number of passes in the homogenizer (Huan et al., 2017; Li et al., 2019; Wu et al., 2020). According to the fibrillation degree, the fibers can be morphologically categorized into three types of fibers: squashed cellulose, incomplete or complete nanofibrillated cellulose (Yuan et al., 2021). The squashed cellulose exhibits the typical band feature microsized in diameter. This banded cellulose acts as a barrier between droplets and prevents droplets from coalescing. Incompletely and completely nanofibrillated cellulose create a layer that connects adjacent oil droplets, forming a droplet-fiber network structure. However, for completely fibrillated cellulose, a denser layer is created promoting the stabilization of emulsion.

The preparation of Pickering emulsions is conventionally performed at lab scale using batch technologies, such as rotor-stator homogenization (Costa et al., 2018; Sanchez-Salvador et al., 2019; He et al., 2020). Rotor-stator homogenizers consist of a stationary hollow casing (the stator) with a rotating shaft inside (the rotor) that creates a pressure differential, drawing the fluid in and out the small space between the rotor and the stator. Due to the extreme change in velocity that happens in this gap, the fluid is subjected to high shear forces that promote the reduction of the droplet's size and stabilization of the emulsion. However, this

technique results in large-size droplets, high energy consumption, high heat release, and a difficult industrial scale-up (Ribeiro et al., 2021). One continuous mode approach to scale up the production of Pickering emulsions is the use of NETmix mesostructured reactor. NETmix was developed at LSRE-LCM, Faculty of Engineering University of Porto (FEUP) (Lopes et al., 2005), and has shown potential to produce Pickering emulsions in continuous mode (Ribeiro et al., 2021). At the core of this technology is a network formed by the repetition of unit cells, each consisting of a chamber connected to two inlet and two outlet channels oriented at 45° from the main flow direction. Contact and consequent mixing between the fluids fed through the inlets occurs in the chambers. The mixture is then split between the outlets and fed to the following chamber (Lopes et al., 2005).

This technology is a solution with higher energy efficiency, easy to scale up, and with full control of the process conditions, when compared to other standard processes. Scale-up is ensured by numbering up NETmix units, guaranteeing the same mixing conditions and high-volume scale production.

In NETmix, the parameter that has the most influence in mixing is the channel's Reynolds number (Re), given by

$$\mathrm{Re} = \frac{\rho\, \upsilon\, d_{\mathrm{h}}}{\mu} \tag{1}$$

where ρ (kg m^{-3}) and μ (Pa·s) are the density and the viscosity of the liquid streams, respectively, υ is the average velocity in the channels (m s^{-1}), and d_{h} the channels' hydraulic diameter (m).

According to previous studies, mixing in the chambers occurs above Re of 150, the channel's critical Reynolds number. For these conditions, there is the formation of a self-sustainable chaotic flow regime able to mix the two liquid streams efficiently (Fonte et al., 2013).

The use of NETmix for the production of emulsions is quite promising since the dynamic flow regime generated in this mesomixer enables the easy control of droplet size, assuring the effective temperature control, which is not controlled in traditional batch reactors (e.g. rotor-stator homogenizers) (Ribeiro et al., 2021).

This paper proposes the use of the high-yield biomass, containing micro and nano cellulose fibrils, (LCMNFs) to stabilize Pickering emulsions for food applications. The main novelties are first the scale-up of the production of stable Pickering emulsions in continuous mode; second, the complete valorization of leek trimmings, which are usually thrown away despite being edible. This treatment does not use chemical treatments and is low cost, making them suitable for food applications. According to FoodData Central of U.S. Department of Agriculture, leek has a low percentage of fat. Thus, leek trimmings are perfect for adding flavour to calorie-controlled diet. The potential applications of these Pickering emulsions in food industries are vegan sauces or butter to seasoning.

Experimental Methods

Materials

The oil phase used was sunflower oil, purchased from a local supermarket, whereas distilled water was used as the aqueous phase. LCB pulps containing LCMNFs were obtained from leek leaves' trimmings, provided by a local greengrocer's shop from Madrid, following a previously described methodology (Sanchez-Salvador et al., 2022). In the preparation of the fibers, no chemical pre-treatments were used, thus avoiding the use of chemicals; leek trimmings were dried, milled, and blended (DMB) and then fibrillated at 600 bar. Two homogenization sequences were considered, at low consistency (LC) and high consistency (HC). The consistency, i.e. the solid content of each pulp of leek, was obtained from

$$\text{consistency (wt.\%)} = \frac{m_{\mathrm{humid}}}{m_{\mathrm{dry}}} \times 100 \tag{2}$$

where m_{humid} is the mass of humid samples and m_{dry} is the mass of oven-dried samples at ~70 °C for 12 h. As Table 1 shows, in both cases, the consistencies used are much higher than traditional CNFs with a solid content of around 1 wt.%.

- HPH-*x*-LC: where *x* corresponds to number of passes in the HPH; $x = 3, 6$, and 9 were analysed for lower consistency DMB leek at 600 bar;
- HPH-*x*-HC: where *x* corresponds to 3, 6, and 9 for higher consistency DMB leek at 600 bar.

LCB pulps containing LCMNFs were characterized using transmittance, aspect ratio, and polymerization degree. Each pulp was first diluted at 0.1 wt.% to determine the transmittance. The measurements were performed at a wavelength of 600 nm on a uniSPEC 4 UV-Visible spectrophotometer (LLG, Meckenheim, Germany). Distilled water was used as reference fluid. The increase in transmittance with the homogenization passes shows an increase in the number of smaller particles, which is pronounced when LCB pulps are homogenized at higher consistency (Levanič et al., 2022).

The aspect ratio was determined from a simplified gel point (GP) methodology described by Sanchez-Salvador et al. (2021). GP is usually obtained from the derivative at the origin of an experimental curve of CNF concentration (c_{o}) vs. ratio of sediment height (H_{s}) to initial suspension height (H_{o}); here, the following simplification was used

Table 1 Characterization of LCB pulps containing LCMNFs from leek leaves' trimmings

	Amount of solids through HPH (%)	Transmittance (%)	Aspect ratio (L/D)	Polymerization degree (monomers)
Low consistency (LC)				
HPH-3-LC	3.65 ± 0.11	7.5 ± 0.1	42 ± 1	288 ± 2
HPH-6-LC	3.64 ± 0.02	9.5 ± 0.1	44 ± 1	287 ± 4
HPH-9-LC	3.64 ± 0.02	9.5 ± 0.1	46 ± 1	279 ± 5
High consistency (HC)				
HPH-3-HC	5.47 ± 0.01	18.7 ± 0.2	40 ± 2	289 ± 2
HPH-6-HC	5.44 ± 0.05	19.6 ± 0.1	41 ± 1	290 ± 10
HPH-9-HC	5.46 ± 0.02	20.0 ± 0.1	42 ± 1	296 ± 6

$$\mathrm{GP}\ (\mathrm{k\ gm^{-3}}) = \lim_{\frac{H_s}{H_o}\to 0}\left(\frac{dc_o}{d\left(\frac{H_s}{H_o}\right)}\right) \approx \frac{c_o(i) - c_o(0)}{\left(\frac{H_s}{H_o}(i)\right) - \left(\frac{H_s}{H_o}(0)\right)} = \frac{c_o(i)}{\left(\frac{H_s}{H_o}(i)\right)} \tag{3}$$

AR was then determined according to

$$\mathrm{AR} = 5.9\left(\frac{\mathrm{GP}}{1000}\right)^{-0.5} \tag{4}$$

assuming a density of fibers of 1500 kg m^{-3} and the crowding number theory (Sanchez-Salvador et al., 2021; Varanasi et al., 2013).

The polymerization degree (PD) was determined from the limiting viscosity number (intrinsic viscosity), according to the ISO 5351 standard (2010). The pulps were diluted in cupriethylenediamine (CED) solution, and the elution time of the 0.5 wt.% sample was measured with a capillary viscometer. The elution time of a reference sample prepared with distilled water and CED was also determined. The ratio of the elution time of fibers (t) and the reference (t_o) samples with the ratio of their viscosity (η and η_o, respectively) according to

$$\frac{\eta}{\eta_o} = \frac{t}{t_o} \tag{5}$$

For a given ratio between η and η_o, the limiting viscosity number $[\eta]$ of the diluted sample was determined according to Martin's equation,

$$\log\,[\eta] = \log\frac{\eta - \eta_o}{\eta_o c} - k[\eta]c_{PD} \tag{6}$$

where k is an empirical constant, which is 0.13 for the cellulose-CED system, and c_{PD} is the exact concentration of pulp-CED sample

PD was then calculated using the Staudinger-Mark-Houwink equation,

$$[\eta] = K_{PD} \cdot \mathrm{PD}^a \tag{7}$$

where K_{PD} and a are parameters specific to the polymer-solvent system. For the cellulose-CED system, K_{PD} and a vary according to

- if PD < 950, $K_{PD} = 0.42$ mL g^{-1} and $a = 1$;
- if PD > 950, $K_{PD} = 2.28$ mL $g.^{-1}$ and $a = 0.76$

Table 1 shows the results for the transmittance, aspect ratio, and polymerization degree for the different consistencies. The increase in transmittance with the homogenization passes shows an increase of the number of smaller particles, which is pronounced when LCB pulps are homogenized at higher consistency. The aspect ratio that measures the relation between length and diameter increases with the homogenization passes from an initial value of 31 ± 3 before homogenization, which indicates fibrillation during HPH. Table 1 shows that the aspect ratio is considered an intermediate value when compared with the results from Kalashnikova et al. (2013). Therefore, it is not expected that in Pickering emulsions, the particles are adsorbed at the interface as cellulose nanocrystals. High-consistency LCMNFs present lower aspect ratios which indicate that also HPH produces the shortening of fibers. Finally, the polymerization degree with a value of 336 ± 22 before homogenization is reduced with the HPH in a similar way in both cases with scarce differences with the number of passes.

Conditions of LCB Pulp Production for Pickering Emulsions Application

Pickering emulsions were prepared using LCB pulps containing LCMNFs collected after different numbers of passes of HPH for the different homogenization sequences. The O/W ratio and the LCB content in the aqueous phase were fixed during these experiments at O/W 40/60 wt.%, LCB 2.25 wt.%.

Emulsification was carried out in a rotor-stator homogenizer T 25 digital ULTRA-TURRAX (IKA, Staufen, Germany) at 16 000 rpm for 3 min. They were then stored in a graduated cylinder at room temperature. The best homogenization sequence and the respective optimal number of HPH passes were chosen according to emulsion stability after 48 h. The volume of the water (V_{water}), oil (V_{oil}), and emulsion ($V_{emulsion}$) phases was measured and emulsion stability was expressed by EI, given by

$$\text{EI}\ (\%) = \frac{V_{\text{emulsion}}}{V_{\text{total}}} \tag{8}$$

where V_{total} is the total volume of the sample.

According to stability results, the chosen pulp was observed by SEM. The sample was oven-dried at ~ 100 °C for 3 h before the analysis. It was then placed on pins with carbon tapes and observed on a desktop Phenom ProX Desktop SEM (Thermo Fisher Scientific, Massachusetts, EUA).

Preparation of the Pickering Emulsions in Batch Mode

Pickering emulsion preparation comprised three steps: dispersion of the fibers in the aqueous phase for 1 min, followed by injection of the oil phase ($t_{\text{injection}}$), and additional stirring to ensure homogenization (t_{stirring}=$t_{\text{injection}}$). Emulsification was carried out at 11 000 rpm in a rotor–stator homogenizer Miccra D-9 (Miccra GmbH, Heitersheim, Germany). The oil was injected through a feeding channel using a peristaltic pump at 240 rpm (~31 mL min^{-1}).

Different LCMNF contents in the aqueous phase and O/W ratios were tested (Table 2). The content of LCB ranged from 1.0 wt.% to its maximum content in the aqueous phase, that is, using the original pulp. The lower consistencies were obtained by dilution of the LCB pulp with water. The O/W ratio ranged from 20/80 to 40/60 wt.%.

Preparation of the Pickering Emulsions in Continuous Mode

Pickering emulsions were produced in continuous mode using the most stable formulations previously determined in batch mode. A NETmix set-up (Fig. 1), with 25 rows and 8 columns, chambers' diameter of 3.3 mm, and channels' hydraulic diameter of 0.5 mm, was used. Before feeding to the NETmix reactor, the oil, water, and LCB were mixed for 1 min in a magnetic stirrer. Then, the mixture was fed to the NETmix reactor, which was set to operate in recirculation mode, using one pump to adjust the flow rate and assure Re > 150 during the experiment.

Characterization of the Pickering Emulsions

Pickering emulsions type, i.e. O/W or W/O emulsions, was predicted by determining contact angle θ and checked from drop test. The stability of all formulations was evaluated by visual inspection. Moreover, emulsions were characterized in terms of morphology using microscopy techniques such as optical microcopy, confocal laser scanning microscopy, and cryo-scanning electron microscopy.

Table 2 Pickering emulsions: LCB content and O/W ratio

O/W ratio / wt.%	LCB content / wt.%
20/80	2.0 | 3.0 | 4.0 | 4.8[a]
30/70	1.0 | 1.5 | 2.0 | 2.5 | 3.0 | 3.5 | 4.2[a]
40/60	1.0 | 1.5 | 2.0 | 2.5 | 3.0 | 3.6[a]

[a]Maximum content in the aqueous phase

Contact Angle (θ) Measurements

A sample of the leek pulp was dried in an oven at 100 °C for 3 h. The resulting powder was pressed into pellets with a diameter of 13 mm and a thickness of ~ 1 mm using a hydraulic press (PerkinElmer) at 10 tonnes. Measurements of θ were performed through a sensible-drop method on an optical tensiometer Theta (Biolin Scientific). A droplet of distilled water (5 µL) was released on pellets surfaced using a high-precision injector and recorded with the high-speed video camera of the equipment. The contact angles for the left- and right-hand sides of the droplet were determined by the software One Attension using the Laplace-Young equation. Results are expressed as the average measurements for different repetitions.

Drop Test

Two drops of each Pickering emulsion were added to the water and oil phases, respectively. According to their behaviour, emulsions were classified as oil-in-water, if emulsion droplets dispersed in water, or water-in-oil, if the opposite occurred.

Visual Inspection

Pickering emulsions formulations of Table 2. were analysed visually to determine their stability. Images were captured after 48 h of production. Stability was expressed by EI (Eq. 2).

Optical Microscopy (OM) Analysis

A drop of emulsion was placed on a microscope slide, covered with a coverslip, and viewed under 10 × magnification. An Axiotech 100 HD optical microscope and a microscope camera AxioCam 105 colour (Zeiss Microscopy, Jena, Germany) were used. Image processing was performed with Zen (2.3 blue edition) software.

Confocal Laser Scanning Microscopy (CLSM) Analysis

CLSM analysis was done using a LEICA TCS-SP5 AOBS (Leica Microsystems, Germany) to visualize the fibers placement at the O/W interface. Each sample

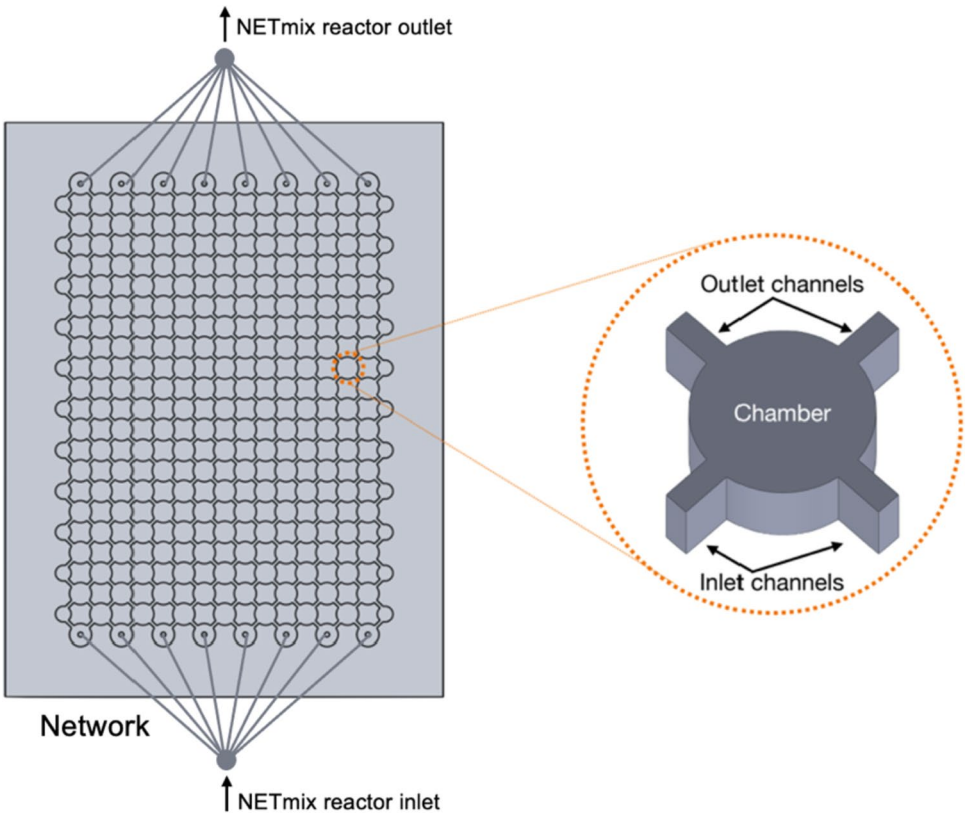

Fig. 1 Schematic representation of the NETmix reactor's network of unit cells and of a single unit cell structure

(3 mL) was stained with a mixture of fluorescent dyes dissolved in isopropyl alcohol (0.3 mL): Nile red at 0.1 w/v%, to dye the fibers, and Nile blue at 0.1 w/v%, to dye the oil droplets. The dyed emulsions were placed on a slide (40 µL) and excited at 488 nm (Nile red) and 633 nm (Nile blue).

Cryo-Scanning Electron Microscopy (cryo-SEM) Analysis

Cryo-SEM analysis was performed using a JEOL JSM 6301F/ Oxford INCA Energy 350/ Gatan Alto 2500. The samples were rapidly cooled (plunging it into sub-cooled nitrogen – slush nitrogen) and transferred under vacuum to the cold stage of the preparation chamber. They were fractured, sublimated (4 min at -90 °C), and coated with Au/Pd (60 s). Then, the samples were transferred into the SEM chamber and observed at -150 °C.

Rheological Characterization

Rheological studies on the viscous and viscoelastic behaviour of Pickering emulsions were performed using a rheometer MCR 92 (Anton Paar, Graz, Austria) with a parallel plate. The zero gap was defined at 0.5 mm and the temperature at 20 C for all measurements. The viscosity curve, i.e. the viscosity of emulsions (η) in function of the shear rate ($\dot{\gamma}$), was measured for a shear rate range from 10 to 300 s^{-1}. The yield stress of emulsions was determined from the flow curve, i.e. the shear stress (τ) in function of $\dot{\gamma}$. The studied range of τ was from 1 to 50 Pa. The linear viscoelastic region (LVR) was also determined by amplitude sweep, considering a shear strain (γ) in the range of 0.01 to 100% and a fixed angular frequency (ω) of 10 rad s^{-1}. LVR region indicates the shear strain where the test can be performed without destroying the structure. The amplitude sweep tests are presented as a plot of storage modulus (G') and loss modulus (G'') in function of γ. After the identification of LVR, a frequency sweep test was performed for ω in the range of 10 to 100 rad s^1 and a fixed shear strain within the LVR. The frequency tests are presented as a plot of G' and G'' in function of ω.

Data Processing Methods

In this work, the data analysis was carried out from the average and the standard deviation of the duplicates. Regarding images, the MO images were processed using the software ZEN 2 to set the scale bars. CLSM image processing was performed using LASX software and ImageJ, and the Cryo-SEM and SEM images were reported as captured by the software. No image editing process (i.e. brightness, saturation, contrast) was made in these images.

Results and Discussion

Concerning the final objective of producing Pickering emulsions in continuous mode using LCB obtained from leek, the optimal conditions (number of HPH passes and consistency) to obtain the stabilizing pulp, and the most stable Pickering emulsions formulations in batch mode were studied. According to the stability results of emulsions produced in a batch mode, emulsions were produced using the NETmix technology.

A preliminary study of the best conditions to produce the LCMNF pulp based on the stability of emulsions is reported in the "Conditions of LCB Pulp Production for Pickering Emulsions Application" section. In the following sections, the analysis of emulsions was based on the evaluation of their type, characterization of their morphology, and mechanism of stabilization. Each analysis was made simultaneously for the batch and continuous processes.

Conditions of LCB Pulp Production for Pickering Emulsions Application

The best conditions to produce the LCB pulp containing LCMNF were determined considering its application to stabilize Pickering emulsions. For this study, the O/W ratio was set at 40/60 wt.% and the LCMNFs in the aqueous phase at 2.25 wt.%; emulsions were prepared varying the parameters to be optimized, i.e. the number of HPH passes and the consistency of the pulp during HPH. These results are reported from duplicates with an error lower than 5% for each phase. After 48 h, stability was evaluated according to phase distribution and the corresponding EI. Figure 2 shows a sketch of the distribution of oil (black), emulsion (grey), and water (white) and the respective EI after 48 h.

The results in Fig. 2 show that an emulsion phase is present after 48 h for all pulps, proving that LCMNF in leek pulp can act as a Pickering stabilizer. Although the pulp contains other components in its composition, the main contribution for the stabilization goes to cellulose since it carries the largest percentage.

An aqueous layer was formed below the emulsion phase for all samples tested. Additionally, in some of the emulsions (0 and 9 HPH passes for HPH-*x*-LC; 0 for HPH-*x*-HC), an oil layer was formed on top of the emulsion phase. Furthermore, even at the highest degree of fibrillation tested, for this formulation, there was not a completely stable emulsion, i.e. with EI = 100 wt.%.

For HPH-*x*-LC, EI increased from 0 to 6 HPH passes. The increase in the number of homogenization passes led to the reduction of the LCB size, increasing the aspect ratio (see Table 1), and increasing the proportion of LCMNFs in the leek pulp. This reduction in LCB size facilitates the

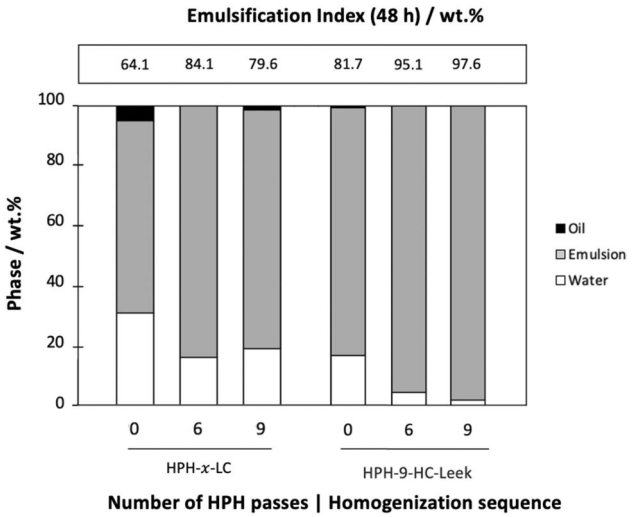

Fig. 2 Conditions for LCB pulp production: phase distribution and EI 48 h after production (O/W 40/60 wt.%; LCB 2.25 wt.%)

emulsion between the oil and the water phase, producing oil droplets surrounded by LCMNFs, avoiding the coalescence. However, from 6 to 9 passes, there was no significant change. For HPH-*x*-HC, a similar tendency was observed, with the EI increasing significantly from 0 to 6 HPH passes with just a small increase from 6 to 9 passes. These results are in accordance with a previous study that also showed that after 6 HPH passes there were no significant changes in properties such as degree of polymerization, aspect ratio, fibers' diameter range, and branching index (Sanchez-Salvador et al., 2022). Thus, due to the higher energy demand involved in performing 9 passes and since it does not provide substantial advantages for Pickering emulsion stabilization, 6 passes were considered the optimal number of HPH passes.

Concerning consistency, HPH-6-HC has the advantage of having spent less energy than HPH-6-LC to homogenize the same initial amount of raw material. For these sequences, the EI analysis at 6 passes shows a considerably higher result for HPH-6-HC (95.1 wt.%) compared to HPH-6-LC (84.1 wt.%). A higher content of solids in the homogenizer facilitates the defibrillation degrees promoting the nano and microfibril content, and higher transmittance according to Table 1. Thus, higher consistencies will ensure the emulsion stability and so, HPH-6-HC was selected for the following stability studies.

For the LCB pulp prepared at HC and 6 passes, the morphology of the LCMNFs was observed from SEM images (Fig. 3), where it is observed that fibers look like thin lamellae of LCMNF, i.e. the shape is similar to the squashed cellulose described in Yuan et al. (2021). This is in line with the results of aspect ratios in Table 1 and the

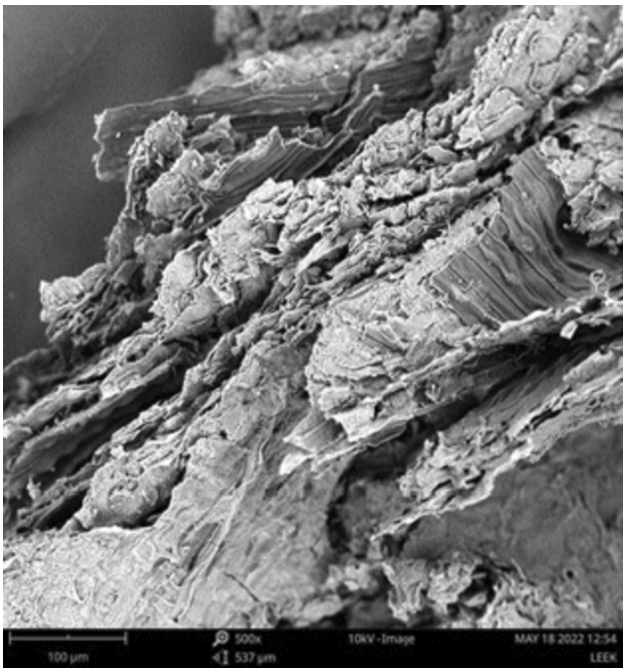

Fig. 3 SEM characterization of the LCMNFs contained in the LCB pulp prepared at HC and 6 passes with a magnification of 500×

research in Kalashnikova et al. (2013), where it is reported that for larger aspect ratios, leek trimmings can exhibit a band feature.

Sanchez-Salvador et al. (2022) describe chemically the leek trimmings. It is chemically composed of 31 wt.% of cellulose, 12 wt.% of hemicellulose, 25 wt.% of lignin, 12% of pectin, 11% of ash, and 9% of extractives on a dry basis. Since the component with higher content is cellulose, and no purification process to isolate cellulose was performed, the fibers are called hereafter cellulosic fibers.

Pickering Emulsions Stability Study

The LCB pulp obtained at HC and 6 passes of HPH was used to prepare different formulations of Pickering emulsions in batch mode. The aim was to determine the best formulations in terms of stability for later production in continuous mode using the NETmix technology as an initial proof of concept. O/W ratios of 20/80, 30/70, and 40/60 wt.% were tested at different LCB in the aqueous phase.

Figure 4 shows the emulsion, oil, and water phase distribution 48 h after emulsification and the corresponding EI. Stability results are in agreement with previous studies (Sanchez-Salvador et al., 2019; Lu et al., 2020), where it is reported that the increase of the emulsion phase is favoured by the increase of CMFs, i.e. in this case of LCB. For 20/80 and 30/70 wt.% O/W ratios, two different formulations resulted in EI > 90 wt.%: the one at maximum LCB and the one below. For 40/60 wt.% O/W ratio, only the formulation at maximum LCB exhibited EI > 90 wt.%. Only for the emulsions at maximum LCB there is no separation of the aqueous phase at the bottom of the vial. Meanwhile, for all formulations, an oil layer was formed on the top, which indicates that the LCB seems to not be enough to stabilize the oil droplets, resulting in their coalescence. To avoid this, a higher amount of LCB would be required, which the limiting consistency of the pulp does not allow.

The stability results that were used to represent the phase distribution and to calculate the respective EI after

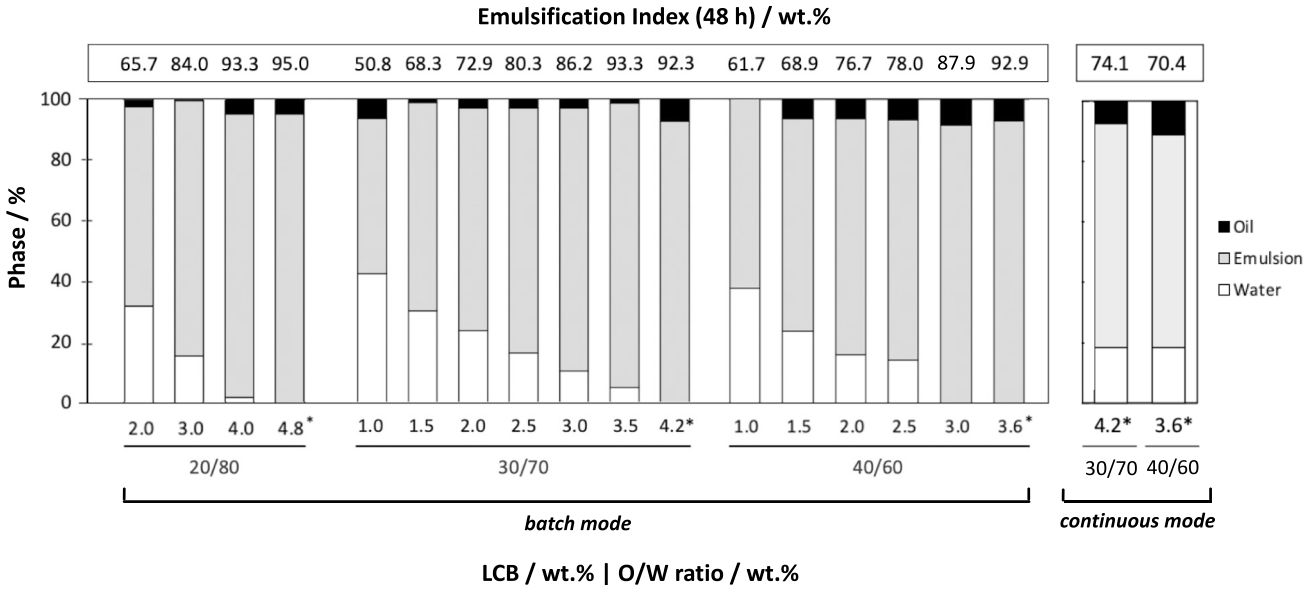

Fig. 4 Pickering emulsions stability 48 h after production: phase distribution and EI of emulsions produced in batch mode and continuous mode

48 h (Fig. 4) were obtained by visual inspection of the different formulations. Figure 5 shows photographs used for the visual inspection after 48 h of the emulsions containing maximum LCB for each O/W ratio, which were identified as the most stable formulations.

Following the batch results, Pickering emulsions were produced in continuous mode, using formulations with O/W 30/70 wt.%, LCB 4.2* wt.% and O/W 40/60 wt.%, LCB 3.6* wt.%. To ensure Re > 150 at the inlet of the NETmix reactor, the flow rate throughout the process was adjusted to 85 and 73 mL min^{-1}, respectively, for each formulation, corresponding to Re of 270 and 224. The NETmix reactor operated in recirculation mode for 12 min, corresponding to 15 and 13 cycles for the O/W 30/70 wt.%, LCB 4.2* wt.% and O/W 40/60 wt.%, LCB 3.6* wt.% formulations, respectively.

The phase distribution after 48 h is shown in Fig. 4 and the corresponding images after visual inspection in Fig. 5. As observed, after 48 h both formulations produced in the NETmix reactor resulted in the formation of an oil layer on the top of the vial, as previously reported for the batch preparations. In addition, an aqueous layer at the bottom was visible. Consequently, the EI was significantly lower when compared with the one obtained in batch mode for the same formulation, evidencing a higher coalescence of droplets. Nevertheless, the results obtained in the NETmix reactor are a proof of concept for producing Pickering emulsions with leek LCB in continuous mode. This is a relevant result since the LCMNFs contained in the LCB pulp have a different shape and size from the hydroxyapatite solid particles tested in previous works (Ribeiro et al., 2021), which are spherical with an average diameter of 18 mm.

Morphology of the Pickering Emulsions and Stabilization Mechanism

The contact angle measurement of 72.8° ± 4.8° indicated that the produced emulsions are of the oil-in-water type (Fig. 6a), which was also confirmed from the drop test (Fig. 6b).

These results are also in agreement with the images observed from CLSM analysis (Fig. 7). Since the oil phase was stained with Nile Red and LCMNFs with Nile Blue, the green fluorescence in the images enables the identification of oil droplets, while the red fluorescence shows where the fibers are located. Moreover, due to the different colouring of the phases, the CLSM technique evidences the LCMNFs' role at the O/W interface.

In all CLSM images, it is possible to identify bundles of cellulosic fibers surrounding oil droplets of spherical shape and irregular size. These bundles enable the creation of a matrix around the oil droplets that covers their surface, avoiding the droplets' coalescence. This stabilization mechanism is also observed for other sources of cellulosic fibers, such as plant cellulosic microfibers (Nomena et al., 2018; Qi et al., 2021) and mangosteen rind (Winuprasith & Suphantharika, 2015).

Due to the irregular shape of LCMNF and the fragile structure (Fig. 3), the fibers are unevenly positioned, resulting in a heterogeneous oil droplet sizes. Irregular sized and shaped droplets surrounded by the LCMNFs are also visible in the OM images taken after emulsification (Fig. 7). Previous works using nanohydroxyapatite (Ribeiro et al., 2022) and apple pomace LCB (Lu et al., 2020) have reported that smaller oil droplets enable better stability results over time. For each shear rate applied by the rotor-stator, i.e. each rotor-stator speed, oil droplets of equal dimensions should be

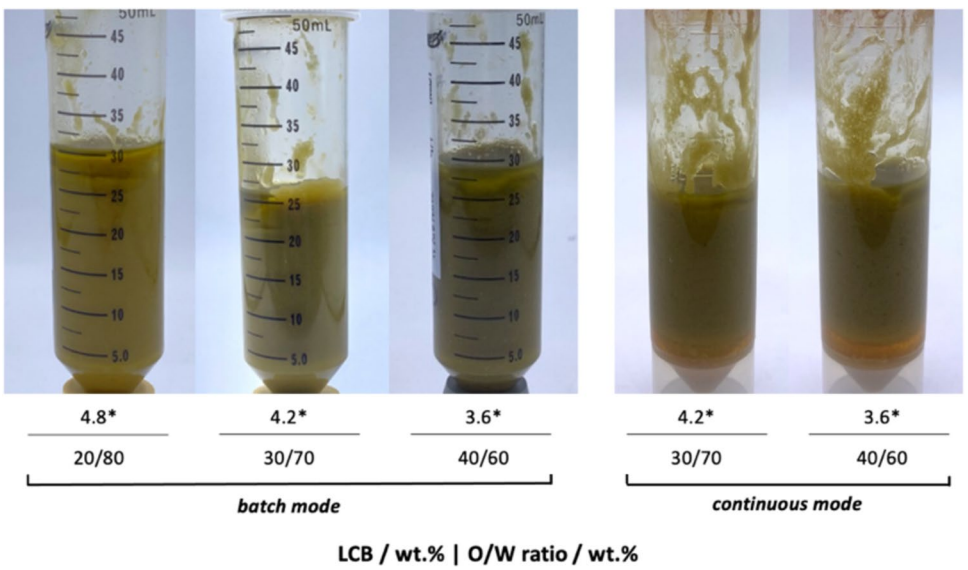

Fig. 5 Pickering emulsions stability 48 h after production: photographs used for visual inspection of emulsion produced in batch mode and continuous mode

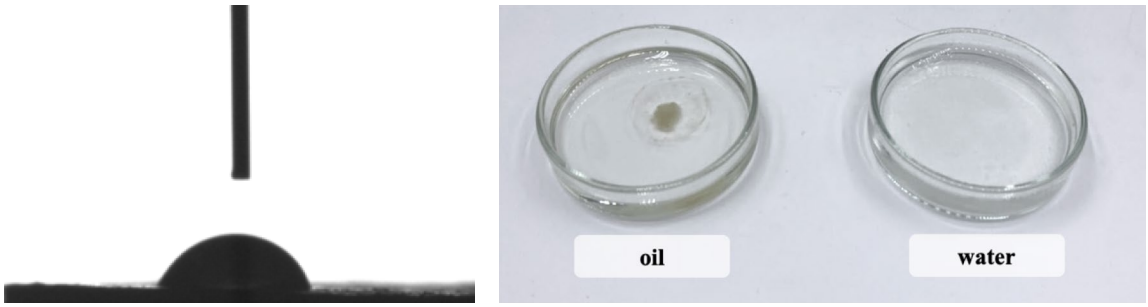

Fig. 6 Emulsion type determination: **a** contact angle measurement; **b** drop test in oil and water (O/W 40/60 wt.%, LCB 1.0 wt.%)

obtained, independently of the O/W ratio. Thus, variations in size are indicators of the coalescence of oil droplets when there are not enough solid particles available to completely cover the O/W interface of the smaller droplets.

In addition to the OM images after emulsification shown in Fig. 7, the analysis was performed after 48 h to compare the emulsion droplets formed in batch and in continuous mode due to the observed inconsistency of stability. The

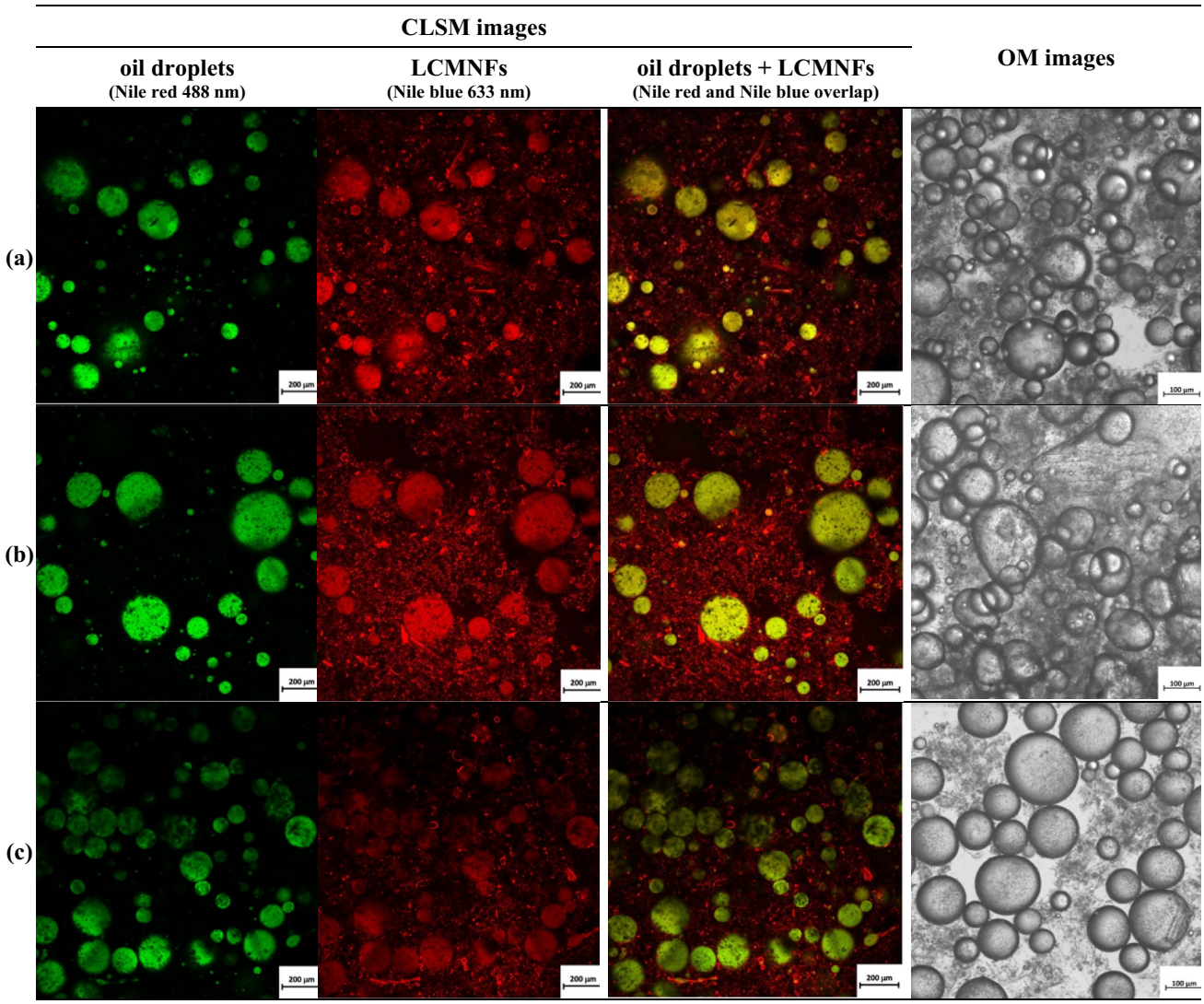

Fig. 7 CLSM and OM (10× magnification) images 0 h after production in batch mode **a** O/W 20/80 wt.%, LCB 4.8* wt.%; **b** O/W 30/70 wt.%, LCB 4.2* wt.%; **c** O/W 40/60 wt.%, LCB 3.6* wt.%

results are shown in Fig. 8 and highlight a clear increase in the droplet size. In batch mode, droplets of even larger size than after production are observed, whereas in continuous mode, the emulsion phase consists of oil droplets with much smaller dimensions and a more regular circular shape.

As batch emulsions have much larger droplet sizes than the emulsions produced in continuous mode, the surface area that needs to be covered by the LCMNFs network is smaller. Thus, for emulsions produced in continuous mode to achieve comparable stability to the batch mode results after 48 h, a higher amount of LCMNFs, and therefore more concentrated LCB suspensions would be required to cover the larger surface area formed by the smaller droplets and avoid their coalescence.

The difference in droplet sizes reported between batch and continuous mode relates to the difference in the shear rate applied during emulsification. In batch, the shear rate ($\dot{\gamma}_{batch}$) corresponds to 7.6×10^4 s^{-1} as given by

$$\dot{\gamma}_{batch}\left(s^{-1}\right) = \frac{\pi\ \omega\ r}{30h} \tag{9}$$

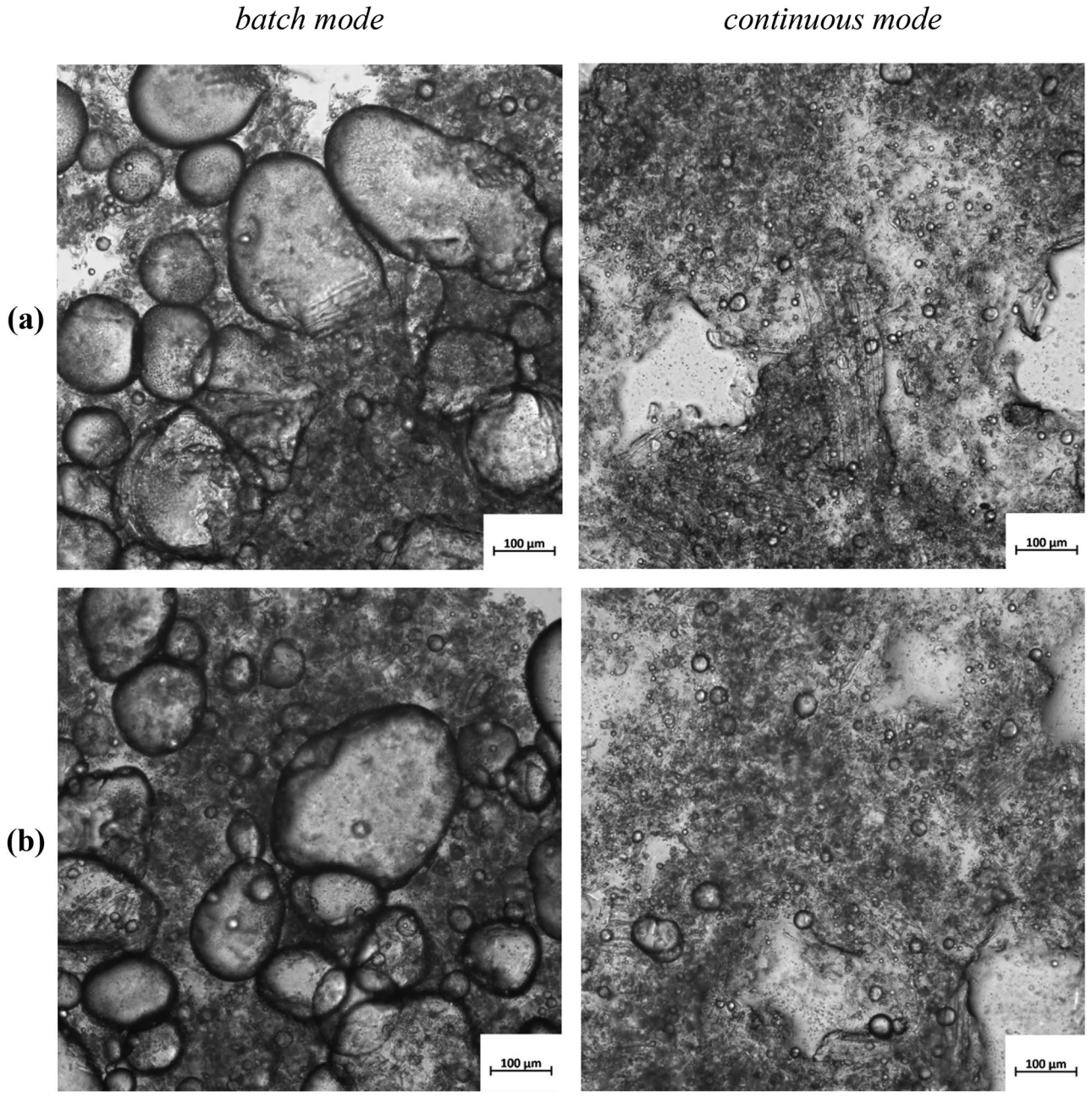

Fig. 8 OM images (10× magnification) 48 h after production in batch and continuous mode for formulations **a** O/W 30/70 wt.%, LCB 4.2* wt.%; **b** O/W 40/60 wt.%, LCB 3.6* wt.%

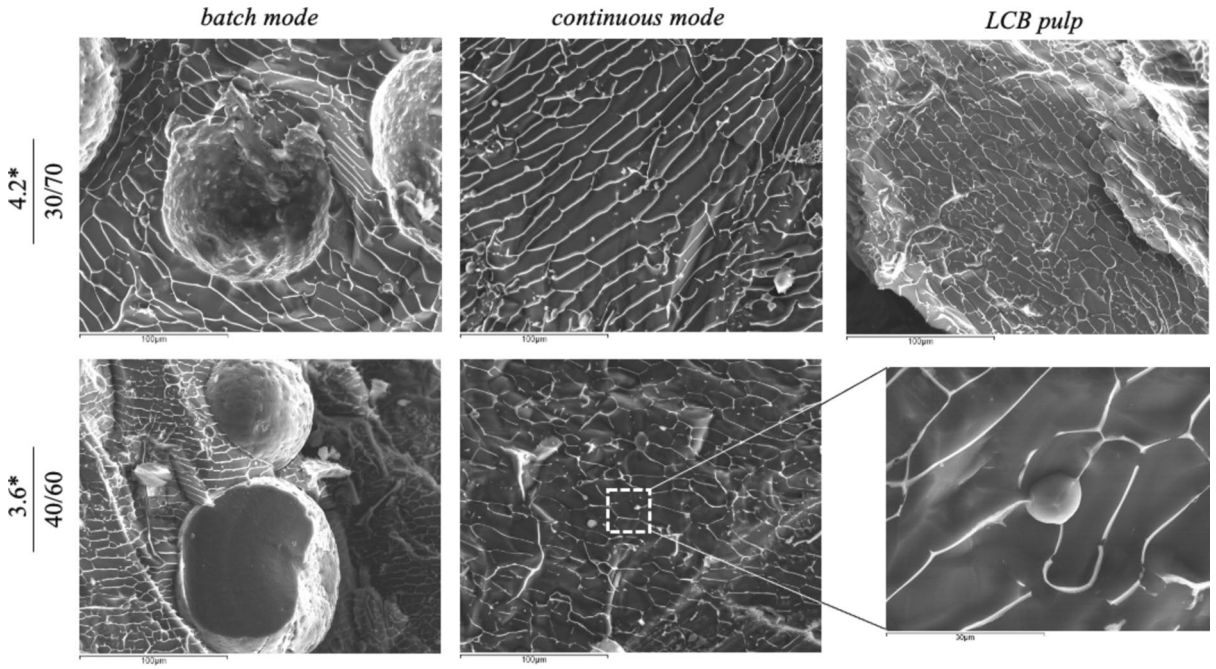

Fig. 9 Cryo-SEM images: LCB pulp and batch and continuous mode Pickering emulsions 48 h after production

where ω is the rotational speed, r is the rotor's radius, and h is the width between rotor and stator.

On the other hand, emulsification is subject to larger shear rates in the NETmix reactor ($\dot{\gamma}_{\mathrm{NETmix}}$), equal to $42 \times 10^4\ \mathrm{s}^{-1}$, according to

$$\dot{\gamma}_{\mathrm{NETmix}}\left(\mathrm{s}^{-1}\right) = \frac{6\upsilon}{d} \tag{10}$$

where υ is the average velocity in the NETmix channels and d is their diameter. As a result, the larger shear rates result in oil droplets of lower diameter in continuous mode.

Additionally, cryo-SEM images of the emulsions were obtained and are shown in Fig. 9, where individual droplets covered by a network of fibers can be observed, corroborating the matrix stabilization mechanism. These cryo-SEM images are similar to SEM pictures reported in Yuan et al. (2021), where it is shown that banded cellulose acts as a barrier between droplets, preventing the coalescence of droplets. It is also observed that droplets clung to the broad surface of the squashed cellulose, as previously reported by Yuan et al. (2021).

The difference in droplet size between the batch and continuous modes is also evidenced by this technique. Therefore, from the characterization presented in this work, namely OM, CLSM and Cryo-SEM images, it is clear that the mechanisms for the emulsions' stabilization are based on the formation of a cellulosic fibers' matrix. The stabilization by particles only occurs for higher fibrillation degrees, requiring more energy in the preparation of fibers.

Rheological Characterization of Batch Mode Emulsions

Rheological properties of the Pickering emulsions produced in batch mode at maximum consistency were analysed since they can influence the emulsions' performance, appearance, and storage stability.

Figure 10a shows the flow curve, that is, the emulsion viscosity, η versus the shear rate, $\dot{\gamma}$. The viscosity decreases with the increase of shear rate, which indicates the non-Newtonian behaviour of the emulsions. However, for higher shear rates, the viscosity does not decrease so abruptly. The highest viscosity was achieved for O/W 20/80 wt.%, LCB 4.8 wt.%.

Pickering emulsions usually start to flow only after the applied stress exceeds a critical value, i.e. yield stress. Below the yield stress, samples deform elastically, and above it, they deform permanently, and its behaviour is similar to a liquid. Yield stress values can be determined from the interception of the flow curve with the yy axis in Fig. 10b and are shown in Table 3. The highest yield stress (21 Pa) is reported for the formulation with the highest EI after 48 h. (Table 3)

Figure 10c shows the amplitude sweep test, which is represented by G' and G'' versus the shear strain, γ. G' represents the elastic portion of the viscoelastic behaviour, whereas G'' represents the viscous portion. For all emulsions, G' is always greater than G'' at low γ. As the shear strain increases, an intersection point between G' and G'' is observed, that corresponds to the shear strain at which deformation of emulsions occurs. The linear viscoelastic

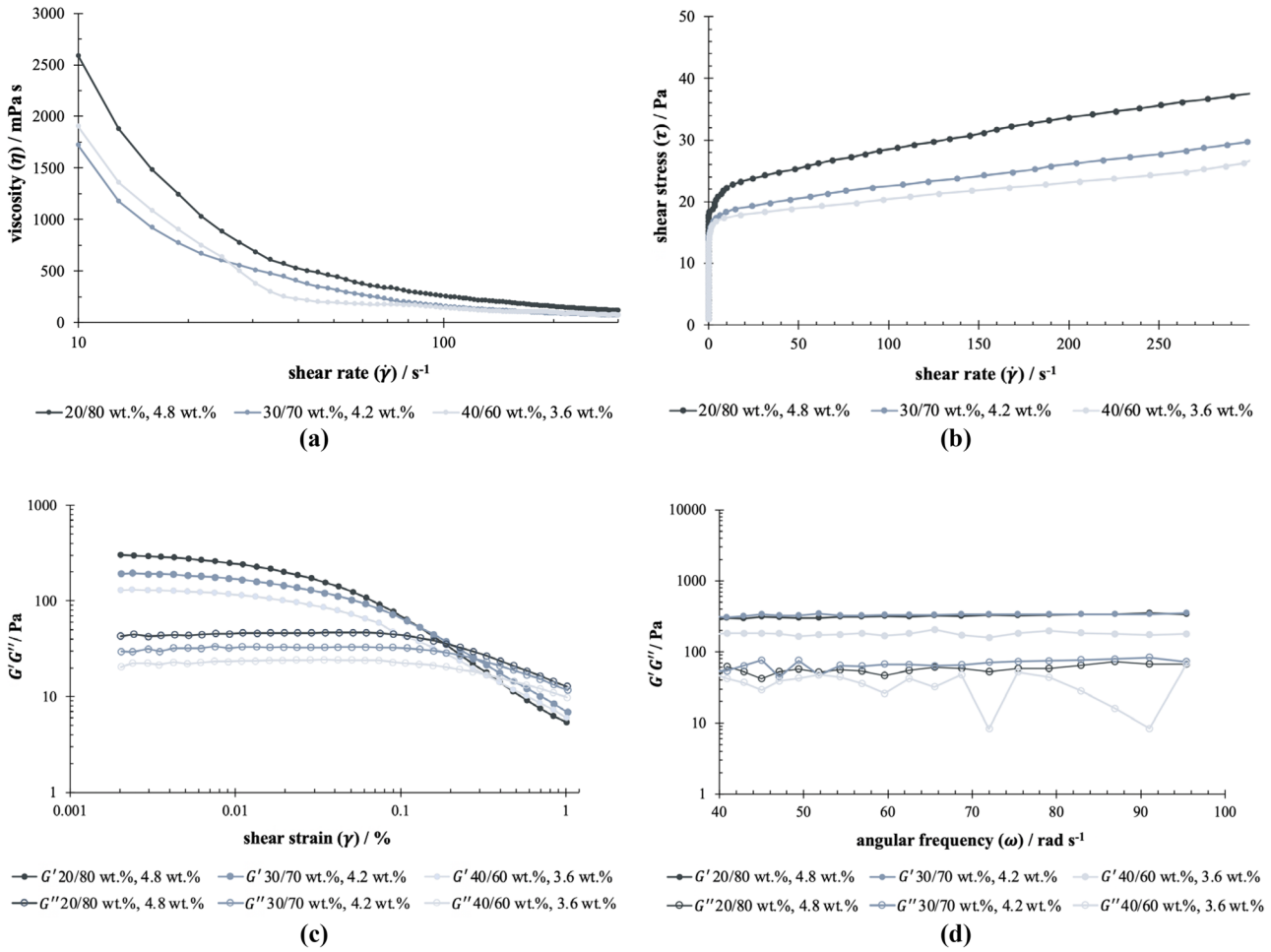

Fig. 10 Rheological characterization of batch mode emulsions at maximum LCB: **a** viscosity versus shear rate; **b** shear stress versus shear rate; **c** storage modulus (G') and loss modulus (G'') versus shear strain; **d** storage modulus (G') and loss modulus (G'') versus angular frequency

region (LVR) corresponds to the shear strain range before the interception of G' and G'' and in this region, the moduli of O/W 20/80 wt.%, LCB 4.8 wt.% is higher, which relates once again to its higher stability.

At 0.01% shear strain, all Pickering emulsions analysed are within LVR. Thus, the shear strain was fixed at that value for the dynamic frequency sweep measurements. Figure 10d shows the frequency sweep test, that is, G' and G'' versus the angular frequency, ω. Dynamic measurements are important to observe the emulsions' behaviour to an external deformation that is a periodic function of time within the non-destructive deformation range. High frequencies are used to simulate fast motion on short timescales, while low frequencies simulate slow motion on long timescales or at rest (Mezger, 2018). As observed in Fig. 9d, both moduli are mostly independent of the frequency over the tested frequency range (40–100 rad s^{-1}). For O/W 40/60 wt.%, LCB 3.6 wt.%, frequency dependence is observed for G''. In addition, G' is greater than G'', evidencing that the emulsions behaviour is predominantly elastic, i.e. solid-state dominant, which is consistent with the development of gel-like networks [1].

Table 3 Rheological characterization of batch mode emulsions at maximum LCB: yield stress

O/W ratio / wt.%	LCB / wt.%	Yield stress / Pa
20/80	4.8*	21
30/70	4.2*	18
40/60	3.6*	16

[1] Gels are solid-like materials with at least two components, one of which is a liquid, where > G''. Ross-Murphy, S. B. (1994). Rheological characterization of polymer gels and networks. *Polymer Gels and Networks*, *2,* 229–237.

Conclusions

This work proposes the use of leek trimmings as particles for Pickering emulsions. Leek trimmings are perfectly edible but currently, they are considered waste. Since they are fat-free, their addition to food will add flavour and contribute to a calorie-controlled diet. O/W Pickering emulsions were successfully stabilized with high-yield LCB pulps from leek trimmings containing LCMNFs, using both batch and continuous mode processes. Since the fibers treatment does not involve the use of chemicals, they can be widely used for the preparation of food-grade Pickering emulsions. Potential applications of these emulsions in the food industry are in vegan sauces or butter for seasoning.

In batch mode, the Pickering emulsions were produced using a rotor-stator homogenizer, promoting the blending of sunflower oil, water, and the LCB pulp. In the continuous process, the sunflower oil and water are continuously fed to the NETmix reactor, a technology developed at the University of Porto.

In batch mode, an EI over 92 wt.% was achieved after 48 h for all O/W ratios studied (20/80, 30/70, and 40/60 wt.%) at the optimal dosage. As observed from OM, CLSM, and cryo-SEM images, the LCMNFs contained in the LCB pulp formed a barrel of fibers capable of enclosing the oil droplets, avoiding their coalescence.

However, the production of the most stable batch formulations at O/W ratios of 30/70 wt.% (LCB 4.2* wt.%) and 40/60 wt.% (LCB 3.6* wt.%) gave lower stability results (EI over 70 wt.%) in continuous mode. MO and cryo-SEM images show that the droplet size is larger in batch than in continuous mode, due to the higher shear rate generated in the NETmix reactor. Since the droplet size is larger in batch mode, the surface area that needs to be covered by the LCMNFs network is smaller.

Therefore, the proof of concept shows the potential of using fiber solid particles to produce Pickering emulsions with vegetable wastes in the NETmix reactor although further studies are required to improve their stability. The continuous production using NETmix reactor ensures their compatibility to the industrial manufacturing processes.

Glossary

CLSM	confocal laser scanning microscopy
CMFs	cellulose microfibrils
CNFs	cellulose nanofibrils
Cryo-SEM	cryo-scanning electron microscopy
DMB	dried, milled, and blended
EI	emulsification index
HC	high consistency
HPH	high-pressure homogenizer
LC	low consistency
LCB	lignocellulosic biomass
LCMNFs	lignocellulose micro and nanofibrils
LVR	linear viscoelastic region
O/W	oil/water
OM	optical microscopy
SEM	scanning electron microscopy

Author Contribution Mariana P. Marques: Investigation, Validation, Methodology, Visualization, Writing – original draft; José Luis Sanchez-Salvador: Supervision, Conceptualization, Investigation, Validation, Writing – review & editing. M. Concepcion Monte: Supervision, Conceptualization, Resources, Formal analysis. Angeles Blanco: Supervision, Conceptualization, Formal analysis, Resources, Investigation, Validation, Writing – review & editing. Ricardo J. Santos: Conceptualization, Formal analysis, Resources, Investigation, Validation, Writing – review & editing. Madalena M. Dias: Resources, Writing – review & editing. Yaidelin A. Manrique: Supervision, Conceptualization, Investigation, Validation, Writing – review & editing. Margarida S.C.A. Brito: Supervision, Conceptualization, Formal analysis, Resources, Investigation, Validation, Writing – review & editing.

Funding Open access funding provided by FCT|FCCN (b-on). This work was financially supported by Project S4Hort_Soil&Food (NORTE-01-0145-FEDER-000074), supported by Norte Portugal Regional Operational Programme (NORTE 2020), under the PORTUGAL 2020 Partnership Agreement, through the European Regional Development Fund (ERDF); UIDB/50020/2020 and UIDP/50020/2020 (LSRE-LCM), UIDB/00511/2020 and UIDP/00511/2020 (LEPABE), and LA/P/0045/2020 (ALiCE), funded by national funds through FCT/MCTES (PIDDAC); project RETOPROSOST 2-CM-P2018/EMT4459 Sustainable Production in Madrid Community (UCM). The authors thank the Centro de Materiais da Universidade do Porto (CEMUP) and Instituto de Investigação e Inovação em Saúde (i3S) for the services provided with cryo-SEM and CLSM analysis, respectively.

Data Availability All data generated or analysed during this study are included in this published article.

Declarations

Competing Interests The authors declare no competing interests.

References

Akcicek, A., Karasu, S., Bozkurt, F., & Kayacan, S. (2022). Egg yolk-free vegan mayonnaise preparation from Pickering emulsion

stabilized by gum nanoparticles with or without loading olive pomace extracts. *ACS Omega, 7*, 26316–26327.

Albert, C., Beladjine, M., Tsapis, N., Fattal, E., Agnely, F., & Huang, N. (2019). Pickering emulsions: Preparation processes, key parameters governing their properties and potential for pharmaceutical applications. *Journal of Controlled Release, 309*, 302–332.

Balea, A. (2017). *Celulosa Nanofibrilada y su Aplicación en la Industria Papelera para la Mejora de Productos Reciclados*. Universidad Complutense de Madrid.

Balea Martin, A., Blanco, A., Delgado-Aguilar, M., Monte, M., Tarrés, Q., Fuente, E., Mutjé, P., & Negro, C. (2021). Nanocellulose characterization challenges. *BioResources, 16*, 4382–4410.

Binks, B. P., & Lumsdon, S. O. (2000). Influence of particle wettability on the type and stability of surfactant-free emulsions. *Langmuir, 16*(23), 8622–8631.

Blanco, A., Monte, M. C., Campano, C., Balea, A., Merayo, N., & Negro, C. (2018). *Chapter 5 - Nanocellulose for industrial use: Cellulose nanofibers (CNF), cellulose nanocrystals (CNC), and bacterial cellulose (BC)* (pp. 74–126). Elsevier.

Chen, B., Zhao, X., Yang, G., Cai, Y., Zhao, M., Zhao Q., & Van der Meeren, P. (2023). Stabilization of emulsions with high physical stability using ultrasonic autoclaving alkaline-treated insoluble soybean fiber. *Food and Bioprocess Technology.*

Chen, L., Ao, F., Ge, X., & Shen, W. (2020). Food-grade pickering emulsions: Preparation, stabilization and applications. *Molecules, 25*, 3202.

Chen, Y., Zhang, H., Feng, X., Ma, L., Zhang, Y., & Dai, H. (2021). Lignocellulose nanocrystals from pineapple peel: Preparation, characterization and application as efficient Pickering emulsion stabilizers. *Food Research International, 150*, 110738.

Costa, A. L. R., Gomes, A., Tibolla, H., Menegalli, F. C., & Cunha, R. L. (2018). Cellulose nanofibers from banana peels as a Pickering emulsifier: High-energy emulsification processes. *Carbohydrate Polymers, 194*, 122–131.

de Folter, J. W. J., van Ruijven, M. W. M., & Velikov, K. P. (2012). Oil-in-water Pickering emulsions stabilized by colloidal particles from the water-insoluble protein zein. *Soft Matter, 8*, 6807–6815.

Fonte, C. M., Leblebici, M. E., Dias, M. M., & Lopes, J. C. B. (2013). The NETmix reactor: Pressure drop measurements and 3D CFD modeling. *Chemical Engineering Research and Design, 91*, 2250–2258.

Guo, S., Li, X., Kuang, Y., Liao, J., Liu, K., Li, J., Mo, L., He, S., Zhu, W., Song, J., Song, T., & Rojas, O. J. (2021). Residual lignin in cellulose nanofibrils enhances the interfacial stabilization of Pickering emulsions. *Carbohydrate Polymers, 253*, 117223.

He, K., Li, Q., Li, Y., Li, B., & Liu, S. (2020). Water-insoluble dietary fibers from bamboo shoot used as plant food particles for the stabilization of O/W Pickering emulsion. *Food Chemistry, 310*, 125925.

Huan, S., Yokota, S., Bai, L., Ago, M., Borghei, M., Kondo, T., & Rojas, O. J. (2017). Formulation and composition effects in phase transitions of emulsions costabilized by cellulose nanofibrils and an ionic surfactant. *Biomacromolecules, 18*(12), 4393–4404.

ISO 5351. (2010). *Pulps—determination of limiting viscosity number in cupri-ethylenediamine (CED) solution*. ISO: Geneva, Switzerland, 2010.

Jiang, Y., Li, F., Li, D., Sun-Waterhouse, D., & Huang, Q. (2019). Zein/pectin nanoparticle-stabilized sesame oil Pickering emulsions: Sustainable bioactive carriers and healthy alternatives to sesame paste. *Food and Bioprocess Technology, 12*(12), 1982–1992.

Jimenez-Lopez, C., Fraga-Corral, M., Carpena, M., Garcia-Oliveira, P., Echave, J., Pereira, A. G., Lourenco-Lopes, C., Prieto, M. A., & Simal-Gandara, J. (2020). Agriculture waste valorisation as a source of antioxidant phenolic compounds within a circular and sustainable bioeconomy. *Food & Function, 11*, 4853–4877.

Kalashnikova, I., Bizot, H., Bertoncini, P., Cathala, B., & Capron, I. (2013). Cellulosic nanorods of various aspect ratios for oil in water Pickering emulsions. *Soft Matter, 9*(3), 952–959.

Levanič, J., Svedström, K., Liljeström, V., Šernek, M., Osojnik Črnivec, I. G., Poklar Ulrih, N., & Haapala, A. (2022). Cellulose fiber and nanofibril characteristics in a continuous sono-assisted process for production of TEMPO-oxidized nanofibrillated cellulose. *Cellulose, 29*(17), 9121–9142.

Li, C., Li, Y., Sun, P., & Yang, C. (2013). Pickering emulsions stabilized by native starch granules. *Colloids and Surfaces a: Physicochemical and Engineering Aspects, 431*, 142–149.

Li, Q., Wang, Y., Wu, Y., He, K., Li, Y., Luo, X., Li, B., Wang, C., & Liu, S. (2019). Flexible cellulose nanofibrils as novel pickering stabilizers: The emulsifying property and packing behavior. *Food Hydrocolloids, 88*, 180–189.

Li, X., Li, J., Kuang, Y., Guo, S., Mo, L., & Ni, Y. (2019). Stabilization of Pickering emulsions with cellulose nanofibers derived from oil palm fruit bunch. *Cellulose, 27*(2), 839–851.

Liang, H.-N., & Tang, C.-H. (2014). Pea protein exhibits a novel Pickering stabilization for oil-in-water emulsions at pH 3.0. *LWT - Food Science and Technology, 58*, 463–469.

Liu, G., Li, W., Qin, X., & Zhong, Q. (2020). Pickering emulsions stabilized by amphiphilic anisotropic nanofibrils of glycated whey proteins. *Food Hydrocolloids, 101*.

Lopes, J. C., Laranjeira, P. E., Dias, M. M., & Martins, A. A. (2005). Network mixer and related mixing process. F. d. E. d. U. d. Porto.

Lu, Z., Ye, F., Zhou, G., Gao, R., Qin, D., & Zhao, G. (2020). Micronized apple pomace as a novel emulsifier for food O/W Pickering emulsion. *Food Chemistry, 330*, 127325.

Maingret, V., Courregelongue, C., Schmitt, V., & Heroguez, V. (2020). Dextran-based nanoparticles to formulate pH-responsive Pickering emulsions: A fully degradable vector at a day scale. *Biomacromolecules, 21*, 5358–5368.

Marto, J., Nunes, A., Martins, A. M., Carvalheira, J., Prazeres, P., Gonçalves, L., Marques, A., Lucas, A., & Ribeiro, H. M. (2020). Pickering emulsions stabilized by calcium carbonate particles: A new topical formulation. *Cosmetics , 7*(62).

Mateo, S., Peinado, S., Morillas-Gutiérrez, F., La Rubia,M. D., & Moya, A. J. (2021). Nanocellulose from agricultural wastes: Products and applications—A review. *Processes, 9*.

Mezger, T. (2018). Applied Rheology – With Joe Flow on Rheology Road.

Miao, C., Atifi, S., & Hamad, W. Y. (2020). Properties and stabilization mechanism of oil-in-water Pickering emulsions stabilized by cellulose filaments. *Carbohydrate Polymers, 248*, 116775.

Negro, C., Balea Martin, A., Sanchez-Salvador, J., Campano, C., Fuente, E., Monte, M., & Blanco, A. (2020). Nanocellulose and its potential use for Sustainable Industrial Applications. *Latin American Applied Research - an International Journal, 50*, 59–64.

Nomena, E. M., Remijn, C., Rogier, F., van der Vaart, M., Voudouris, P., & Velikov, K. P. (2018). Unravelling the mechanism of stabilization and microstructure of oil-in-water emulsions by native cellulose microfibrils in primary plant cells dispersions. *ACS Applied Bio Materials, 1*(5), 1440–1447.

Olorunsola, E. O., Akpabio, E. I., Adedokun,M. O., & Ajibola, D. O. (2018). Emulsifying properties of hemicelluloses. *Science and Technology Behind Nanoemulsions*, IntechOpen.

Pickering, S. U. (1907). CXCVI.—Emulsions. *Journal of the Chemical Society Transaction, 91*(0), 2001–2021.

Pirozzi, A., Capuano, R., Avolio, R., Gentile, G., Ferrari, G., & Donsi, F. (2021). O/W Pickering emulsions stabilized with cellulose nanofibrils produced through different mechanical treatments. *Foods, 10*(8).

Qi, J.-R., Song, L.-W., Zeng, W.-Q., & Liao, J.-S. (2021). Citrus fiber for the stabilization of O/W emulsion through combination of Pickering effect and fiber-based network. *Food Chemistry, 343*, 128523.

Rao, P., & Rathod, V. (2019). Valorization of food and agricultural waste: A step towards greener future. *The Chemical Record, 19*, 1858–1871.

Rescignano, N., Fortunati, E., Armentano, I., Hernandez, R., Mijangos, C., Pasquino, R., & Kenny, J. M. (2015). Use of alginate, chitosan and cellulose nanocrystals as emulsion stabilizers in the synthesis of biodegradable polymeric nanoparticles. *Journal of Colloid and Interface Science, 445*, 31–39.

Ribeiro, A., Manrique, Y. A., Barreiro, F., Lopes J. C. B., & Dias, M. M. (2021). Continuous production of hydroxyapatite Pickering emulsions using a mesostructured reactor. *Colloids and Surfaces A: Physicochemical and Engineering Aspects, 616.*

Ribeiro, A., Manrique, Y. A., Ferreira, I. C. F. R., Barreiro, M. F., Lopes, J. C. B., & Dias, M. M. (2022). Nanohydroxyapatite (n-HAp) as a pickering stabilizer in oil-in-water (O/W) emulsions: A stability study. *Journal of Dispersion Science and Technology, 43*(6), 814–826.

Ross-Murphy, S. B. (1994). Rheological characterization of polymer gels and networks. *Polymer Gels and Networks, 2*, 229–237.

Saffarionpour, S. (2020). Nanocellulose for stabilization of Pickering emulsions and delivery of nutraceuticals and its interfacial adsorption mechanism. *Food and Bioprocess Technology, 13*(8), 1292–1328.

Sanchez, L. M., Rincón, E., de Haro Niza, J., Martín, R. M., Espinosa, E., & Rodríguez, A. (2023). Vegetable lignocellulosic residues and chitosan as valuable resources in the superabsorbent bio-aerogel development for food conservation. *Food & Bioprocess Technology.*

Sanchez-Salvador, J. L., Balea, A., Monte, M. C., Blanco A, & Negro, C. (2019). Pickering emulsions containing cellulose microfibers produced by mechanical treatments as stabilizer in the food industry. *Applied Sciences 9*(2).

Sanchez-Salvador, J. L., Marques, M. P., Brito, M. S. C. A., Negro, C., Monte, M. C., Manrique, Y. A., Santos, R. J., & Blanco, A. (2022). Valorization of vegetable waste from leek, lettuce, and artichoke to produce highly concentrated lignocellulose micro- and nanofibril suspensions. *Nanomaterials, 12*(24), 4499.

Sanchez-Salvador, J. L., Monte, M. C., Negro, C., Batchelor, W., Garnier, G., & Blanco, A. (2021). Simplification of gel point characterization of cellulose nano and microfiber suspensions. *Cellulose, 28*(11), 6995–7006.

Sharkawy, A., Barreiro M. F., & A. E. Rodrigues (2021). New Pickering emulsions stabilized with chitosan/collagen peptides nanoparticles: Synthesis, characterization and tracking of the nanoparticles after skin application. *Colloids & Surfaces A: Physicochemical & Engineering Aspects, 616.*

Tzoumaki, M. V., Moschakis, T., Kiosseoglou, V., & Biliaderis, C. G. (2011). Oil-in-water emulsions stabilized by chitin nanocrystal particles. *Food Hydrocolloids, 25*, 1521–1529.

Varanasi, S., He, R., & Batchelor, W. (2013). Estimation of cellulose nanofibre aspect ratio from measurements of fibre suspension gel point. *Cellulose, 20*(4), 1885–1896.

Winuprasith, T., & Suphantharika, M. (2015). Properties and stability of oil-in-water emulsions stabilized by microfibrillated cellulose from mangosteen rind. *Food Hydrocolloids, 43*, 690–699.

Wu, J., Zhu, W., Shi, X., Li, Q., Huang, C., Tian, Y., & Wang, S. (2020). Acid-free preparation and characterization of kelp (Laminaria japonica) nanocelluloses and their application in Pickering emulsions. *Carbohydrate Polymers, 236*, 115999.

Ye, F., Miao, M., Jiang, B., Campanella, O. H., Jin, Z., & Zhang, T. (2017). Elucidation of stabilizing oil-in-water Pickering emulsion with different modified maize starch-based nanoparticles. *Food Chemistry, 229*, 152–158.

Yuan, T., Zeng, J., Wang, B., Cheng, Z., & Chen, K. (2021). Pickering emulsion stabilized by cellulosic fibers: Morphological properties-interfacial stabilization-rheological behavior relationships. *Carbohydrate Polymers, 269*, 118339.

Zhang, Y., Zhou, F., Zeng, X., Shen, P., Yuan, D., Zhong, M., Zhao, Q., & Zhao, M. (2022). pH-driven-assembled soy peptide nanoparticles as particulate emulsifier for oil-in-water Pickering emulsion and their potential for encapsulation of vitamin D3. *Food Chemistry, 383*, 132489.

Zongguang, T., Yanping, H., Quangang, Z., Wei, W., Tao, Y., Zhongjian, C., & Yi, L. (2020). Utility of Pickering emulsions in improved oral drug delivery. *Drug Discovery Today, 25*(11).